

Universal Fragility of Spin Glass Ground States under Single Bond Changes

Mutian Shen¹, Gerardo Ortiz², Yang-Yu Liu^{3,4}, Martin Weigel⁵, and Zohar Nussinov^{6,1,7,*}

¹Department of Physics, Washington University, St. Louis, Missouri 63160, USA

²Department of Physics, Indiana University, Bloomington, Indiana 47405, USA


³Channing Division of Network Medicine, Department of Medicine, Brigham and Women's Hospital and Harvard Medical School, Boston, Massachusetts 02115, USA

⁴Center for Artificial Intelligence and Modeling, The Carl R. Woese Institute for Genomic Biology, University of Illinois at Urbana-Champaign, Champaign, Illinois 61801, USA

⁵Institut für Physik, Technische Universität Chemnitz, 09107 Chemnitz, Germany

⁶Rudolf Peierls Centre for Theoretical Physics, University of Oxford, Oxford OX1 3PU, United Kingdom

⁷LPTMC, CNRS-UMR 7600, Sorbonne Université, 4 Place Jussieu, 75252 Paris cedex 05, France

 (Received 16 June 2023; revised 16 March 2024; accepted 30 April 2024; published 11 June 2024)

We consider the effect of perturbing a single bond on ground states of nearest-neighbor Ising spin glasses, with a Gaussian distribution of the coupling constants, across various two- and three-dimensional lattices and regular random graphs. Our results reveal that the ground states are strikingly fragile with respect to such changes. Altering the strength of only a single bond beyond a critical threshold value leads to a new ground state that differs from the original one by a droplet of flipped spins whose boundary and volume diverge with the system size—an effect that is reminiscent of the more familiar phenomenon of disorder chaos. These elementary fractal-boundary *zero-energy droplets* and their composites feature robust characteristics and provide the lowest-energy macroscopic spin-glass excitations. Remarkably, within numerical accuracy, the size of such droplets conforms to a universal power-law distribution with exponents that depend on the spatial dimension of the system. Furthermore, the critical coupling strengths adhere to a stretched exponential distribution that is predominantly determined by the local coordination number.

DOI: [10.1103/PhysRevLett.132.247101](https://doi.org/10.1103/PhysRevLett.132.247101)

Introduction.—Complex systems harboring a plethora of competing low-energy states lie at the forefront of intense investigation across diverse fields in physics, computation, biology, and network science (including long-standing foundational quests associated with the basic character of both real and artificial neural networks and protein folding) [1–5]. Spin glasses are paradigmatic realizations of the venerable challenges posed by these systems. Decades after their discovery, fundamental aspects of spin glasses [1,2,6,7] remain ill understood. Excluding the fully connected Sherrington-Kirkpatrick mean-field model [8] and other soluble theories, e.g., Refs. [9–11], debates concerning the nature of real finite-dimensional spin glasses persist to this day. These systems are commonly described by the nearest-neighbor Edwards-Anderson (EA) model [12]. We will take the physically pertinent (and subtle) continuous real number limit [13] of the EA coupling constants prior to the thermodynamic limit [14]. With unit probability [15], up to a trivial sign flip of all spins (a degeneracy henceforth implicit), the system provably has a unique ground state [13]. While some consensus has emerged regarding the existence and character of the spin-glass phase transition [16–18], at least in Ising systems, with a lower critical dimension between 2 and 3 [19], important questions

remain regarding the spin-glass phase itself: e.g., whether there is an asymptotically nontrivial overlap distribution and a hierarchical structure of metastable states. A central enigma is to what extent the alluring structure of the replica-symmetry breaking (RSB) solution of the mean-field model survives in systems of finite dimensions d . Four descriptions received most attention: (i) the full RSB framework extended to finite dimensions [20], (ii) the droplet scaling theory [21–23], (iii) the trivial–nontrivial (TNT) [24–26], and (iv) the chaotic-pairs (CP) pictures [27,28]. The most distinctive features of these pictures relate to the relevant low-energy excitations. In the RSB phase, such excitations have, asymptotically, an energy of order $O(1)$, independent of system size, and space-filling domain walls appear between pure-state regions. By contrast, conventional droplet scaling predicts energies $\sim \ell^\theta$ for excitations on scale ℓ with a fractal boundary of dimension $d_f < d$ [21–23]. The TNT and CP scenarios feature $O(1)$, $d_f < d$ (TNT) and high-energy ($\theta > 0$), $d_f = d$ excitations (CP) [28], respectively. In numerical studies, such excitations are injected via boundary condition changes applied to systems of linear size L [29]. The corresponding ground-state energy scales as L^θ with θ negative in $d = 2$ and positive when $d \geq 3$ [30–32]. However, since this setup

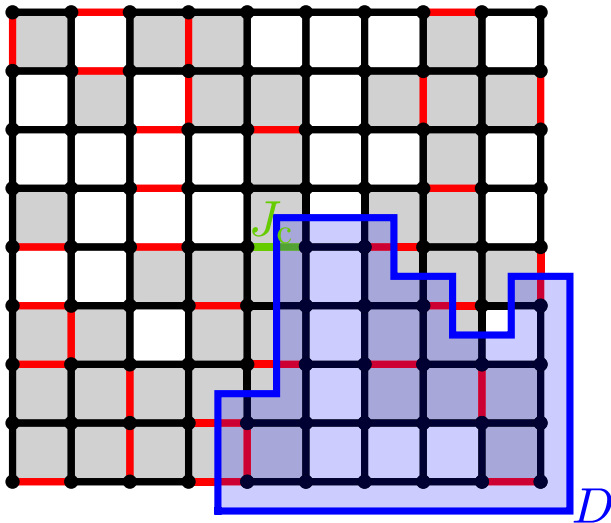


FIG. 1. Illustration of our numerical experiments. Gray and white squares represent frustrated and unfrustrated plaquettes, respectively. Red and black segments represent unsatisfied ($J_{ij}\sigma_i\sigma_j < 0$) and satisfied ($J_{ij}\sigma_i\sigma_j > 0$) bonds. The critical value J_c of the coupling of the central bond (i_0, j_0) (highlighted in green) separates two different ground states that differ by a domain D of flipped spins (shaded region). The boundary links in ∂D are the bisected orthogonal (blue) edges.

requires a macroscopic change of couplings, the resulting excitations might not be representative of low-temperature behaviors. Several studies investigated more local excitations [24,26,33–35] but their behaviors for short-range continuous spin glasses remained somewhat inconclusive.

Zero-energy droplets.—We consider the Gaussian EA Ising model [12] with N spins $\sigma_i = \pm 1$ and Hamiltonian

$$\mathcal{H}_J = -\sum_{\langle ij \rangle} J_{ij} \sigma_i \sigma_j, \quad (1)$$

where $\langle ij \rangle$ denotes nearest neighbors. Here, we assume free boundary conditions. The couplings $\mathcal{J} = \{J_{ij}\}$ are drawn from a Gaussian $\mathcal{P}_J(J_{ij}) = (1/\sqrt{2\pi}) \times \exp(-J_{ij}^2/2)$. Starting from the ground state of a given sample, we vary a *single* coupling constant $J_{i_0 j_0}$ of a bond (i_0, j_0) at the system center from its initial strength J_0 until it reaches a critical value J_c at which a new ground state appears (see Fig. 1). Some properties of such droplets involving single bond changes in the hypercubic EA Ising model [33] were studied analytically in Ref. [28], yet specific results for the physically relevant cases in $d = 2$ and $d = 3$ were not provided. On tuning $J_{i_0 j_0}$, ground states become degenerate at a specific value $J_{i_0 j_0} = J_c$, differing by a domain of flipped spins whose boundary is a contour of zero energy. Previous work referred to the so-formed zero-energy droplet (ZED) as a *critical droplet* [36]. Generally, spins flipped in any domain D (not necessarily a ZED) relative to

those in the ground state are associated with boundary (∂D) energies [37],

$$\Delta E = -2 \sum_{\langle ij \rangle \in \partial D} J_{ij} \sigma_i \sigma_j \geq 0, \quad \partial D = \{\langle ij \rangle | i \notin D, j \in D\}. \quad (2)$$

The following properties can be proven [38,43] (i) If $\Delta E = 0$ (a ZED), the set of flipped spins will contain exactly one of the two endpoints of the central bond [28]. (ii) As $J_{i_0 j_0}$ is continuously varied from $-\infty$ (where the central bond connects two oppositely oriented Ising spins) to ∞ (when the two spins are parallel), there will only be a *single* ground-state transition at the critical coupling $J_{i_0 j_0} = J_c$. Thus, if perturbing $J_{i_0 j_0}$ to a new value generates a new ground state \mathcal{C}' , then this state must differ from the original ground state \mathcal{C} by the very same spins in the ZED appearing when $J_{i_0 j_0} = J_c$ [28]. Furthermore, (iii) the energy associated with a ground-state change (even if the number of flipped spins diverges) incurred by altering a local exchange constant is asymptotically independent of system size if the distribution of the associated critical couplings at which a transition occurs is well defined in the thermodynamic limit. If the distribution of J_c values does not scale with system size (as we indeed verify) then neither will the energy changes.

Multidroplet excitations.—We may vary couplings J_{ij} on general (noncentral) bonds and examine their respective ZEDs to study multidroplet excitations for arbitrary \mathcal{J} . From (2), for general couplings, ΔE vanishes at “criticality” for nontrivial domains when degeneracy appears and is linear in deviations of the coupling constants from their critical values. In the thermodynamic limit, for a continuous distribution \mathcal{P}_J , one can find any finite number of disjoint bonds that are arbitrarily close to their critical values. Thus, in that limit, the critical boundary excitations that we examine and composites of a few such excitations may be of the lowest possible energy. A related result holds for arbitrary energy excitations [38].

Numerical calculations.—We studied ZEDs by computing ground states of the EA Ising model on square, triangular, and honeycomb lattices of linear size $16 \leq L \leq 1024$, cubic lattices with $5 \leq L \leq 12$, body-centered cubic systems with $L = 5, 7$, and z -regular random graphs (RRGs) of coordination numbers $z = 3, 4$, and 6 with $N = 128$ nodes. For each specific lattice or graph, we used between 10^3 and 10^5 bond configurations (disorder samples) for averaging [38]. For planar spin glasses, we used the polynomial-time minimum-weight perfect matching method [44,45] with *Blossom V* [46] to determine exact ground states. For nonplanar systems, an exact branch-and-cut approach (implemented with *Gurobi* [47]) executes brute force tree searches of all possible spin configurations. The code used for this work is publicly available [48].

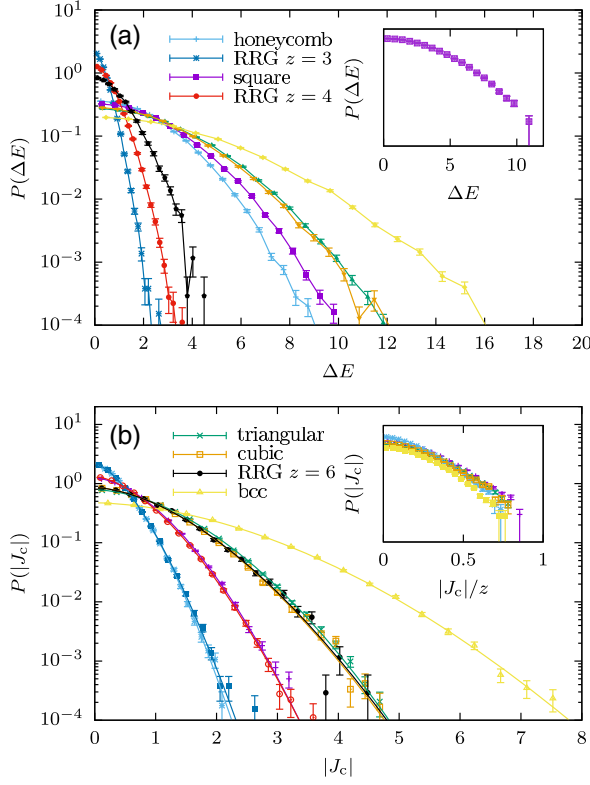


FIG. 2. (The legend is split between both panels, each of which shows all datasets.) (a) Probability densities for the excitation energies ΔE for different lattices and graphs. The inset shows the distributions for square lattices of sizes $L = 16, 64, 256,$ and 1024 (darker shades for larger systems), illustrating that they are almost perfectly independent of system size. (b) Probability densities of the modulus of the critical coupling, $|J_c|$, together with fits of the compressed exponential form (3) to the data. Curves for lattices or graphs of the same coordination number z are nearly indistinguishable. The inset shows the distributions as a function of $|J_c|/z$.

Droplet energies and critical couplings.—When the central coupling $J_{i_0j_0}$ varies from an initial strength of J_0 across J_c to a new value, the corresponding ground state of (1) transitions from \mathcal{C} to \mathcal{C}' . From the perspective of the original system with the initial coupling $J_{i_0j_0} = J_0$, the configuration \mathcal{C}' constitutes an excitation of energy [49] $\Delta E = 2|J_0 - J_c|$ [38,43] above that of the ground state \mathcal{C} . Using the latter relation for ΔE , we inferred J_c by comparing the ground states found for $J_{i_0j_0} \ll 0$ and $J_{i_0j_0} \gg 0$, respectively. In Fig. 2(a), we present excitation energies ΔE for the $d = 2$ and $d = 3$ lattices as well as the RRGs. The distributions are unimodal, peaking close to $\Delta E = 0$, with the energy changes increasing with the lattice (or graph) coordination number z . As the inset shows for the example of the square lattice, the distributions are almost perfectly independent of the system size. Hence there is *no scaling of the excitation energies with system size*. To better understand these distributions, we examined the behavior of the critical couplings J_c . As their

TABLE I. Parameters of the compressed exponential (3), as well as values of the scaling exponents κ_v of Eq. (4) for the droplet volume and κ_s of (5) for the droplet boundary, for the different lattices considered.

Lattice	a_c	β_c	κ_v	κ_s
Honeycomb	2.76(1)	1.58(1)	0.215(2)	0.342(3)
Square	1.187(8)	1.71(1)	0.224(2)	0.346(2)
Triangular	0.523(7)	1.80(1)	0.216(3)	0.336(3)
Simple cubic	0.69(4)	1.55(5)	0.131(6)	0.159(5)
bcc	0.21(1)	1.79(5)	0.116(5)	0.147(7)

probability density is even [38], in Fig. 2(b) we show the distribution of the modulus $|J_c|$. These distributions are well described by a compressed exponential (or stretched Gaussian) [38]

$$P(|J_c|) = k_c \exp(-a_c |J_c|^{\beta_c}), \quad (3)$$

with $1 < \beta_c < 2$. The lines in Fig. 2(b) show fits of this form with the parameters collected in Table I. The typical values for J_c are mostly determined by the lattice or graph coordination number z ; the distributions almost collapse if plotted as a function of $|J_c|/z$, cf. the inset of Fig. 2(b). For instance, data for the ($z = 6$) cubic lattice nearly collapse onto those of the ($z = 6$) triangular lattice. Similarly, the $P(|J_c|)$ distributions for RRGs of fixed coordination $z = 3, 4, 6$ but otherwise random structure match with their counterparts of the honeycomb, square, and triangular lattices, respectively. Deviations are most pronounced for small z . This is particularly apparent for a $z = 2$ graph (i.e., a chain) for which $P(|J_c|) = \delta(|J_c|)$ (since any sign change of $J_{i_0j_0}$ generates a new ground state in which all spins on one side of this bond are flipped with degenerate ground states at $J_{i_0j_0} = 0$). Asymptotically, $P(|J_c|)$ is independent of boundary conditions, although finite-size corrections might be strong [38]. We observed that the probability that the ground state does not change when the initial central coupling is flipped ($J_{i_0j_0} \rightarrow -J_{i_0j_0}$) increases with the density of closed loops [38].

Droplet volumes and boundary areas.—We next study the ZED geometries. In Fig. 3(a), we show the tail distribution of the number $|D|$ of sites (or volume) of these droplets for square lattices of sizes $32 \leq L \leq 1024$. All tails follow a power-law successively extending to larger droplet volumes,

$$P(|D| \geq \mathcal{V}) = 1 - F(\mathcal{V}) = \frac{1}{\mathcal{V}_0^{\kappa_v}} \Omega\left(\frac{\mathcal{V}}{\mathcal{V}_0}\right) \sim k_v \mathcal{V}^{-\kappa_v}, \quad (4)$$

where F is the cumulative distribution and Ω a scaling function. Once the ZEDs become too large, $\mathcal{V} \gtrsim \mathcal{V}_0(L)$, the finite size of the system becomes manifest and the probability plummets far more rapidly with the ZED size.

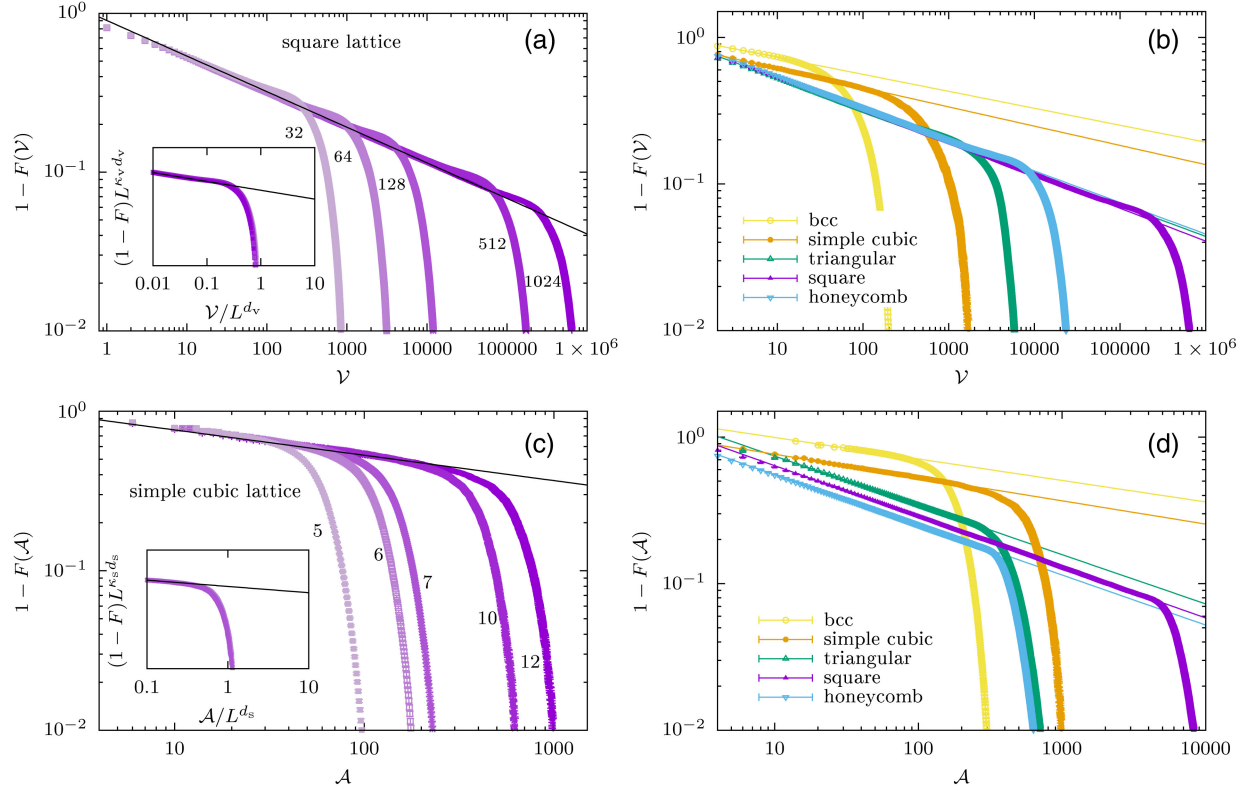


FIG. 3. ZED volume \mathcal{V} and surface area \mathcal{A} distributions. (a) Distribution of ZED volumes for square lattices of sizes $L = 32$ – 1024 (darker shades correspond to larger systems). The inset shows the scaling function Ω of Eq. (4) assuming $\mathcal{V}_0 \sim L^{d_v}$ with $d_v = 1.991(75)$ (see below). (b) Volume distributions for the different lattice types with fits of the power-law form (4). (c) The ZED surface areas for simple cubic lattices of sizes $L = 5$ – 12 . The inset shows Σ of Eq. (5) assuming $\mathcal{A}_0 \sim L^{d_s}$ with $d_s = 2.76(2)$ (see below). (d) Surface area distribution for different lattices with fits (5). For the surface area distribution for the square lattices and the volume distribution for the simple cubic lattices, see Fig. S1 in the Supplemental Material [38].

As is illustrated in Fig. 3(b), we find similar power laws for all considered $d = 2$ and $d = 3$ lattices. The exponent κ_v appears to only depend on the lattice dimension d . Thus, we find the compatible $\kappa_v \approx 0.22$ for the square, triangular, and honeycomb lattices, and $\kappa_v \approx 0.125$ for the simple cubic, and bcc lattices, respectively. The individual fit values appear in Table I. By comparison to their planar counterparts, the more notable differences between the simple cubic and bcc lattices are likely a consequence of the smaller linear sizes in $d = 3$.

The ZED surface areas $|\partial D|$ exhibit a similar power-law distribution

$$P(|\partial D| \geq \mathcal{A}) = 1 - F(\mathcal{A}) = \frac{1}{\mathcal{A}_0^{\kappa_s}} \Sigma\left(\frac{\mathcal{A}}{\mathcal{A}_0}\right) \sim k_s \mathcal{A}^{-\kappa_s}. \quad (5)$$

As seen in Fig. 3(c), deviations from the power-law behavior occur for $\mathcal{A} \gtrsim \mathcal{A}_0(L)$ with $\mathcal{A}_0(L)$ monotonically increasing in L [50]. As Fig. 3(d) illustrates, the exponents κ_s are again universal, depending only on the lattice dimension, cf. the fit parameters in Table I. For RRGs with sparse closed loops, $P(|\partial D| \leq \mathcal{A})$ becomes very sharp. For tree-like graphs (no closed loops), an entire branch of spins

attached to the central bond flips when $J_{i_0 j_0}$ changes sign. Here, the boundary separating the ground states for positive and negative $J_{i_0 j_0}$ is comprised of only one ($|\partial D| = 1$) bond and $P(|\partial D| \leq \mathcal{A})$ increases sharply (a step function). Similarly, a higher exponent κ_s [sharper $P(|\partial D| \leq \mathcal{A})$] appears for lattices of lower spatial dimension d having fewer closed loops (see Table I).

Fractal dimension.—Analyzing, for the square lattice, the scaling of the ZED volume and surface areas with their linear extent ℓ [38], we deduce a volume fractal dimension $d_v = 1.97(3)$ and a surface fractal dimension $d_s = 1.27(1)$ [38]. An alternative analysis using scaling collapses according to Eqs. (4) and (5) yields the compatible estimates $d_v = 1.991(75)$ and $d_s = 1.275(30)$ [38]. Square lattice ZEDs are hence compact (i.e., $d_v \approx d = 2$) with fractal surfaces of Hausdorff dimension compatible with that of domain walls induced by changes of the boundary conditions, $d_{s,DW} = 1.2732(5)$ [51]. This similarity of fractal dimensions is intuitive as the flipping of boundary couplings involved in transitioning from periodic to antiperiodic boundary conditions is akin to a sequence of ZED flips [52]. Indeed, the injection of a domain wall can be viewed as sequentially flipping the bonds, one after the other, along a system

boundary [28,38]. For the cubic lattice, a similar analysis yields $d_v = 3.08(5)$ [20] and $d_s = 2.76(2)$ [15], where the numbers in square brackets indicate the estimated systematic corrections from finite size [38]. Since $d_v \leq d = 3$, this suggests that $d_v \approx d = 3$. Again, d_s is comparable to previous estimates $d_s \approx 2.6$ [25].

Given the cumulative power-law tail distributions of (4) and (5), it is clear that the probability *densities* of volumes and surface areas decay algebraically (with exponents $\kappa_v + 1$ and $\kappa_s + 1$, respectively) implying that the *average* volume $\langle \mathcal{V} \rangle$ and surface area $\langle \mathcal{A} \rangle$ diverge with L . Specifically, the power-law ($\propto \mathcal{V}^{-(\kappa_v+1)}$) regime of the ZED volume distribution implies that $\langle \mathcal{V} \rangle > \int_0^{\mathcal{V}_0} d\mathcal{V} \mathcal{V}^{-\kappa_v} / \int_0^{\mathcal{V}_0} d\mathcal{V} \mathcal{V}^{-(\kappa_v+1)} \propto \mathcal{V}_0$. There are additional $\mathcal{V} > \mathcal{V}_0$ contributions not following the power law (4). The scaling collapse in the inset of Fig. 3(a) illustrates that $\mathcal{V}_0 \sim L^{d_v}$ such that the average volume diverges with L . Likewise, $\langle \mathcal{A} \rangle \sim L^{d_s}$. Hence critical ZEDs are excitations of *divergent volumes (nearly extensive in the system size) with fractal boundaries*.

Discussion.—The ground states of the Gaussian EA Ising model are exceedingly fragile and respond with (ZED) excitations of unbounded size to perturbations of single couplings. We find universal exponents governing the geometrical size of these excitations, the distribution of (“critical”) single couplings, and energies. In the thermodynamic limit, many couplings are inevitably arbitrarily close to being critical such that an infinitesimal amount of energy may create macroscopic system-spanning excitations. All excitations (domain-wall or other) may be associated with ZEDs that appear as exchange constants are sequentially tuned to values that they assume when these excitations arise [38]. The energies of system-spanning $d = 2$ domain-wall excitations of length ℓ vanish as ℓ^θ with $\theta = -0.2793(3) < 0$ [51]. Thus, large ℓ domain-walls in $d = 2$ asymptotically become ZEDs. When keeping the couplings fixed, spin configurations associated with (generally system spanning) single bond ZEDs constitute excitations of energies that do not scale with L . In $d = 3$ or whenever $\theta > 0$, domain-wall excitation energies diverge with increasing L and are thus less relevant for low-temperature physics. In $d = 2$ and $d = 3$ lattices, ZED volume and surface area distributions follow *universal power laws* with finite lattice cutoffs. ZEDs have compact volumes with Hausdorff dimensions $d_v \approx d$ and fractal boundaries $d - 1 < d_s < d$ consistent with domain walls in $d = 2$. The ZED size monotonically increases with external field [38].

Our setup for investigating ZEDs is complementary to that for “disorder chaos” wherein randomness is introduced globally by perturbing all couplings in the system [43,53–60]. This leads to an energy contribution proportional to $\ell^{d_s/2}$. According to droplet theory, the relevant energy scale

is $\Delta E \propto \ell^\theta$, suggesting disorder chaos whenever $d_s/2 > \theta$. By their nature, ZED perturbations (whose existence is guaranteed in the thermodynamic limit) are *always* relevant low-energy excitations.

Since vanishing energy and more general excitations are composites of ZEDs [38], our findings carry important consequences. The defining ZED characteristics impose constraints on the properties of excitations in various pictures. Although finite-size corrections can be strong for spin glasses, the power-law exponents in Table I clearly indicate divergent droplet sizes in $d = 2$ and $d = 3$. The ZEDs are compact with fractal, but not space-filling, boundaries and $O(1)$ energy, thus differing from conventionally considered spin-glass excitations [38], and providing a test for comprehensive spin glass theories.

We thank Daniel Fisher, David A. Huse, Michael A. Moore, Daniel L. Stein, and Gilles Tarjus for discussions and correspondence. Z. N. is grateful to the Leverhulme-Peierls senior researcher Professorship at Oxford supported by a Leverhulme Trust International Professorship grant (No. LIP-2020-014). Part of this work was performed at the Aspen Center for Physics, which is supported by National Science Foundation Grant No. PHY-2210452.

*Corresponding author: zohar@wustl.edu

- [1] M. Mezard, G. Parisi, and M. A. Virasoro, *Spin Glass Theory and Beyond* (World Scientific, Singapore, 1987).
- [2] D. L. Stein and C. M. Newman, *Spin Glasses and Complexity* (Princeton University Press, Princeton, NJ, 2013).
- [3] F. Menczer, S. Fortunato, and C. A. Davis, *A First Course in Network Science* (Cambridge University Press, Cambridge, England, 2020).
- [4] M. Newman, *Networks: An Introduction (second Edition)* (Oxford University Press, New York, 2018).
- [5] J. D. Bryngelson and P. G. Wolynes, Spin glasses and the statistical mechanics of protein folding, *Proc. Natl. Acad. Sci. U.S.A.* **84**, 7425 (1987).
- [6] J. A. Mydosh, *Spin Glasses: An Experimental Introduction* (Taylor and Francis, London, Washington D.C., 1993).
- [7] K. Binder and A. P. Young, Spin glasses: Experimental facts, theoretical concepts, and open questions, *Rev. Mod. Phys.* **58**, 801 (1986).
- [8] D. Sherrington and S. Kirkpatrick, Solvable model of a spin-glass, *Phys. Rev. Lett.* **35**, 1792 (1975).
- [9] B. Derrida, Random-energy model: Limit of a family of disordered systems, *Phys. Rev. Lett.* **45**, 79 (1980).
- [10] B. Derrida, Random-energy model: An exactly solvable model of disordered systems, *Phys. Rev. B* **24**, 2613 (1981).
- [11] D. J. Gross and M. Mezard, The simplest spin-glass, *Nucl. Phys.* **B240**, 431 (1984).
- [12] S. Edwards and P. W. Anderson, Theory of spin glasses, *J. Phys. F* **5**, 965 (1975).
- [13] M.-S. Vaezi, G. Ortiz, M. Weigel, and Z. Nussinov, The binomial spin glass, *Phys. Rev. Lett.* **121**, 080601 (2018).

- [14] A delicate interplay exists between the latter two (continuum coupling and thermodynamic system size) limits. These two limits do not commute with one another [13].
- [15] Degeneracies arise for special values of the coupling constants (a set of measure zero).
- [16] M. Palassini and S. Caracciolo, Universal finite-size scaling functions in the 3D Ising spin glass, *Phys. Rev. Lett.* **82**, 5128 (1999).
- [17] H. G. Katzgraber, M. Körner, and A. P. Young, Universality in three-dimensional Ising spin glasses: A Monte Carlo study, *Phys. Rev. B* **73**, 224432 (2006).
- [18] M. Hasenbusch, A. Pelissetto, and E. Vicari, The critical behavior of 3D Ising glass models: Universality and scaling corrections, *J. Stat. Mech.* (2008) L02001.
- [19] S. Boettcher, Stiffness of the Edwards-Anderson model in all dimensions, *Phys. Rev. Lett.* **95**, 197205 (2005).
- [20] G. Parisi and T. Temesvári, Replica symmetry breaking in and around six dimensions, *Nucl. Phys.* **B858**, 293 (2012).
- [21] W. L. McMillan, Scaling theory of Ising spin glasses, *J. Phys. C* **17**, 3179 (1984).
- [22] D. S. Fisher and D. A. Huse, Equilibrium behavior of the spin-glass ordered phase, *Phys. Rev. B* **38**, 386 (1988).
- [23] A. J. Bray and M. A. Moore, Scaling theory of the ordered phase of spin glasses, in *Heidelberg Colloquium on Glassy Dynamics*, edited by J. L. van Hemmen and I. Morgenstern (Springer, Heidelberg, 1987), p. 121.
- [24] F. Krzakala and O. C. Martin, Spin and link overlaps in three-dimensional spin glasses, *Phys. Rev. Lett.* **85**, 3013 (2000).
- [25] M. Palassini and A. P. Young, Nature of the spin glass state, *Phys. Rev. Lett.* **85**, 3017 (2000).
- [26] F. Houdayer, J. Krzakala, and O. C. Martin, Large-scale low-energy excitations in 3-d spin glasses, *Eur. Phys. J. B* **18**, 467 (2000).
- [27] C. M. Newman and D. L. Stein, Metastate approach to thermodynamic chaos, *Phys. Rev. E* **55**, 5194 (1997).
- [28] C. M. Newman and D. L. Stein, Ground state stability and the nature of the spin glass phase, *Phys. Rev. E* **105**, 044132 (2022).
- [29] M. Cieplak and J. R. Banavar, Sensitivity to boundary conditions of Ising spin-glasses, *Phys. Rev. B* **27**, 293 (1983).
- [30] A. J. Bray and M. A. Moore, Lower critical dimension of Ising spin glasses: A numerical study, *J. Phys. C* **17**, L463 (1984).
- [31] A. K. Hartmann and A. P. Young, Lower critical dimension of Ising spin glasses, *Phys. Rev. B* **64**, 180404(R) (2001).
- [32] S. Boettcher, Stiffness exponents for lattice spin glasses in dimensions $d = 3, \dots, 6$, *Eur. Phys. J. B* **38**, 83 (2004).
- [33] A. K. Hartmann and M. A. Moore, Generating droplets in two-dimensional Ising spin glasses using matching algorithms, *Phys. Rev. B* **69**, 104409 (2004).
- [34] V. Mohanty and A. A. Louis, Robustness and stability of spin-glass ground states to perturbed interactions, *Phys. Rev. E* **107**, 014126 (2023).
- [35] E. Marinari and G. Parisi, Effects of a bulk perturbation on the ground state of 3d Ising spin glasses, *Phys. Rev. Lett.* **86**, 3887 (2001).
- [36] C. M. Newman and D. L. Stein, Nature of ground state incongruence in two-dimensional spin glasses, *Phys. Rev. Lett.* **84**, 3966 (2000).
- [37] Here, σ_j denotes the current spin at site j following the spin inversion. The prefactor of two is a consequence of the sign inversion of the initial $\sigma_i \sigma_j$ following the spin flip in D .
- [38] See Supplemental Material at <http://link.aps.org/supplemental/10.1103/PhysRevLett.132.247101>, which includes Refs. [39–42], for additional analyses relating to the properties of ZEDs.
- [39] O. Melchert, AUTOSCALE.PY—a program for automatic finite-size scaling analyses: A user’s guide, [arXiv:0910.5403](https://arxiv.org/abs/0910.5403).
- [40] J. Houdayer and A. K. Hartmann, Low-temperature behavior of two-dimensional Gaussian Ising spin glasses, *Phys. Rev. B* **70**, 014418 (2004).
- [41] L. Münster and M. Weigel, Cluster percolation in the two-dimensional Ising spin glass, *Phys. Rev. E* **107**, 054103 (2023).
- [42] G. Parisi, Infinite number of order parameters for spin-glasses, *Phys. Rev. Lett.* **43**, 1754 (1979).
- [43] L.-P. Arguin, C. M. Newman, and D. L. Stein, A relation between disorder chaos and incongruent states in spin glasses on Z^d , *Commun. Math. Phys.* **367**, 1019 (2019).
- [44] I. Bieche, R. Maynard, R. Rammal, and J. P. Uhry, On the ground-states of the frustration model of a spin-glass by a matching method of graph-theory, *J. Phys. A* **13**, 2553 (1980).
- [45] C. K. Thomas and A. A. Middleton, Matching Kasteleyn cities for spin glass ground states, *Phys. Rev. B* **76**, 220406(R) (2007).
- [46] V. Kolmogorov, Blossom V: A new implementation of a minimum cost perfect matching algorithm, *Math. Program. Comput.* **1**, 43 (2009).
- [47] Gurobi Optimization, LLC, Gurobi Optimizer Reference Manual (2022).
- [48] <https://github.com/renesmt/ZED>.
- [49] This follows from Eq. (2) and property (ii).
- [50] We further monitor boundary effects and the cutoff \mathcal{A}_0 when using open boundary conditions; on a square lattice, ZED perimeters of odd integer lengths are possible only for $\mathcal{A} > \mathcal{A}_0$ (when ZEDs touch the boundary).
- [51] H. Khoshbakht and M. Weigel, Domain-wall excitations in the two-dimensional Ising spin glass, *Phys. Rev. B* **97**, 064410 (2018).
- [52] As noted, property (ii) following Eq. (2), implies that (a) any nonempty domain D of overturned ground-state spins in a new ground state generated by changing a single bond, e.g., $J_{ij} \rightarrow -J_{ij}$, is identically the same as that of the ZED appearing when (b) J_{ij} is tuned to criticality.
- [53] A. J. Bray and M. A. Moore, Chaotic nature of the spin-glass phase, *Phys. Rev. Lett.* **58**, 57 (1987).
- [54] A. A. Middleton, Energetics and geometry of excitations in random systems, *Phys. Rev. B* **63**, 060202(R) (2001).
- [55] F. Krzakala and J.-P. Bouchaud, Disorder chaos in spin glasses, *Europhys. Lett.* **72**, 472 (2005).
- [56] H. G. Katzgraber and F. Krzakala, Temperature and disorder chaos in three-dimensional Ising spin glasses, *Phys. Rev. Lett.* **98**, 017201 (2007).

- [57] D. Hu, P. Ronhovde, and Z. Nussinov, Phase transitions in random Potts systems and the community detection problem: Spin-glass type and dynamic perspectives, *Philos. Mag.* **92**, 406 (2012).
- [58] W. Wang, J. Machta, and H.G. Katzgraber, Chaos in spin glasses revealed through thermal boundary conditions, *Phys. Rev. B* **92**, 094410 (2015).
- [59] W.-K. Chen and A. Sen, Parisi formula, disorder chaos and fluctuation for the ground state energy in the spherical mixed p-spin models, *Commun. Math. Phys.* **350**, 129 (2017).
- [60] M. Baity-Jesi, E. Calore, A. Cruz, L. A. Fernandez, J. M. Gil-Narvion, I. Gonzalez-Adalid Pemartin, A. Gordillo-Guerrero, D. Iñiguez, A. Maiorano, E. Marinari *et al.*, Temperature chaos is present in off-equilibrium spin-glass dynamics, *Commun. Phys.* **4**, 74 (2021).